

Automated Evaluation of Image Quality in Mammography

Introduction

In digital mammography, the quality of the obtained images plays a crucial role for the diagnosis of breast cancer [1]. In order to assure quality standards for mammographic images, several quality control tests have to be done periodically. More specifically, the following functionalities have to be tested: automated exposure control (AEC), detector uniformity, detection of pixel and line artifacts, detective quantum efficiency (DQE, for more details, see e.g. [2]) and the detector linearity.

An operator has to conduct these tests manually, which is very time consuming. The goal of this work is to support the operator by either automatically assisting the test procedure or even fully automating tests where possible. Our approach brings considerable improvements in the time frame necessary to conduct the aforementioned tests. Additionally, an automated test procedure positively influences the reliability and repeatability of test results.

Several authors considered the assessment of the image quality in digital mammography by defining evaluation criteria on phantoms [3,6,7,10]. However, during these tests, a human operator has to place the phantom on the right position, or has to select suitable regions for measuring the DQE. This interaction is crucial for the image quality assessment process, since errors in the test setup can significantly influence the test results.

Our work presents an approach to assist the operator in performing all five tests. Simple tests like for the detector uniformity were fully automated and need no human interaction at all.

In this paper, we briefly describe our solution to the automation of these tests. Since the test for the detector linearity involves the most complicated processing, we describe this method in detail in the main part of the paper.

Material and Methods

First, we give an overview over the addressed tests and the developed testing framework. Afterwards, we describe in detail the test for the detector linearity.

Testing Framework

The framework for automating and assisting the quality tests consists of solutions for five common problems. The platform we used was a Siemens MAMMOMAT Inspiration digital mammography system. The guidelines for the tests were taken from the Siemens Quality Control Manual [8] and the European Guidelines for the Quality Assurance in Breast Cancer Screening and Diagnosis [4]. Besides the test of the detector linearity (which is described in the next subsection), the following tests were automated.

a) Check of the automated exposure control (AEC): the AEC is a mechanism to minimize the exposure of the patient to radiation while maintaining a sufficiently high image quality. The test setup is as follows: the operator has to align breast phantoms with different transmittance properties on the detection unit. The AEC mask must be within the area of the phantom, should reach as close to its borders as possible and should not contain holes around the center of the mask. The automation of this test involves two steps: we assure the correct phantom placement and we automatically assess the AEC mask.

As a cue for the correct phantom placement, we ensure that the phantom boundaries are within the correct area: we binarize the image, such that phantom pixels are distinguished from background pixels. Then we verify that the bounding box of the binarized image lies within the target area. For the verification of the AEC mask we compare the binarized image with the computed AEC mask. The mask must cover at least 70% of the phantom area. Holes are indirectly determined by summing over the difference of the binarized image and the AEC mask, while weighting center pixels higher than boundary pixels.

b) Check of the detector uniformity: non-uniform intensity distributions are typically compensated with gain correction. We define five regions of interest (ROIs), consisting of one ROI in the center and one ROI per corner of the detector unit. The detector is assumed to be non-uniform if the relative deviation of the mean intensities of all five ROIs and the mean intensity of a single ROI exceed 0.07, in accordance to [8].

c) Detection of pixel and line artifacts: single pixels and whole detector lines can fail during the lifetime of the detector unit. Such pixels respond with consistently too low intensities. The determination of defect pixels is done by measuring the relative deviation D_p of a pixel p from its neighborhood R with a number of pixels N in a flat field image:

$$D_p = \frac{p - \sum_{i=1}^N R_i}{\sum_{i=1}^N R_i} \text{ where } i, N \in \mathbb{N}.$$

Defect rows or columns are determined by counting the number of defect pixels along the x- and y-axis, respectively.

d) Assisted region selection for the DQE computation: for measuring the DQE, the operator has to place a rectangular phantom on the detector plate and hand-select a suitable edge along the phantom. This procedure was automated by preselecting an edge segment on the center of every side of the phantom.

Detector Linearity Test

On our detector used, the Entrance Surface Air Kerma (ESAK) and the obtained image intensities have to be in linear relation. In practice, this requirement must only hold for the typically used range of ESAK. During the test, a dosimeter is used to measure the ESAK for ten different doses. Afterwards, the measured quantities are related to the image intensities in a fixed ROI. In order to obtain reliable results, it is crucial that the sensor of the dosimeter is placed within a specified position on the detector unit, as outlined in Fig. 1., we present a technique for verifying the correct position and orientation of the dosimeter.

We follow an established image registration approach, that accounts for the fact that dosimeters from several manufacturers differ in shape and size. In our experiments, we used the dosimeter Xi by Unfors [9].

Determining the correct orientation of the dosimeter is important, since the sensor position is on one end of the dosimeter (see Fig. 2). We follow a two-stage approach: first, we register the dosimeter in order to obtain the position and orientation up to a 180° twist. In the second step, we register what we call a characteristic component (see Fig. 3) to both ends of the dosimeter, in order to find out the missing 180° rotation.

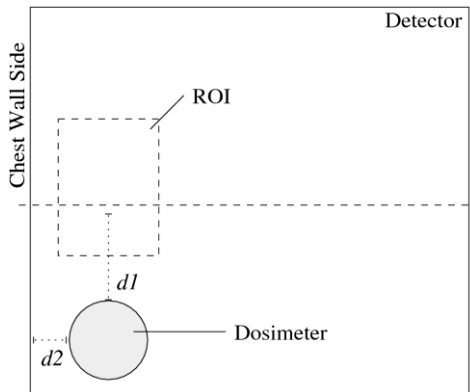


Fig. 1: Linearity test set up.

The template image, we use during the registration, is an exposure of the dosimeter, taken once with a high dose to obtain bright pixel intensities.

As registration framework we have chosen the Insight Segmentation and Registration Toolkit (ITK) [5] which is a standard library for medical image processing.

In the rest of this subsection, we present the details of our methodology. We begin with a general description of our registration method, and afterwards, we describe the first and second registration step.

Registration method

Since the template and the obtained image differ mainly in translation and rotation, it can be described as a rigid 2D transform. There is no need to scale the image as it is assumed that all exposures are taken on the same detector device with constant resolution.

In this work, we use a gradient descent optimizer with bilinear interpolation.

As objective function, we chose the normalized cross-correlation S_{NC} , which is defined as

$$S_{NC}(A, B) = -1 \cdot \frac{\sum_{i=1}^N (A_i \cdot B_i)}{\sqrt{\left(\sum_{i=1}^N A_i^2\right) \cdot \left(\sum_{i=1}^N B_i^2\right)}}$$

with $i, N \in \mathbb{N}$, where A and B are N -dimensional vectors of intensities of the template and an arbitrary image. The metric is minimal and (therefore optimal) if A and B are equal. Preliminary experiments showed that a simpler objective function, e.g. the sum of squared differences, was in our case not applicable, due to sensitivities to the varying image intensities over different doses.

First registration step

If we ignore the wire on the dosimeter there exist two possible solutions that the first registration approach reaches a minimum. One case is the correct matching and the second case the matching rotated by 180° degrees. The last one means that the sensor position (Fig. 2) is on the opposing site. Although this constitutes a local minimum for the metric, the twist results in a wrong estimate of the sensor position.



Fig. 2: Exposure of the dosimeter Xi taken with the Siemens MAMMOMAT Inspiration.

We initialize the gradient descent optimization with a rough estimate of the rotation centers of both images. Since most available dosimeters have a symmetric shape we use a simple algorithm to determine the centroids of the objects. In a preprocessing step each image is binarized with a histogram threshold in order to separate the object from the background. This results in a bimodal histogram with two sharp peaks. The threshold is chosen between both maxima. Then, we project every pixel on the x- and y-axis and determine the centroids on both axes to estimate the centroid of the object. The reference image contains only the dosimeter template and a small neighborhood around it.

Registration of the characteristic component

As shown in Fig 2., the sensor of the dosimeter is not positioned in the center of the device. We applied a second registration step on a characteristic component of the dosimeter in order to remove the local minimum

around the 180° twist. For the dosimeter used in our work we used the wire plug as the template (Fig 3.).

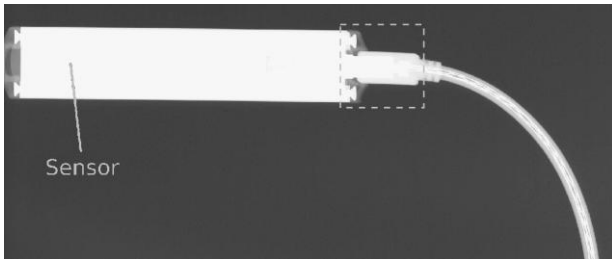


Fig. 3: Registration of the characteristic component (dashed).

In our case, two plausible locations exist for the wire plug, namely the two short sides of the dosimeter. We try to register the wire plug to both ends of the dosimeter and chose the better match according to the normalized cross-correlation result.

For the initialization of the registration, we use the already known translation and rotation parameters of the first step and prior knowledge of the dosimeter size.

The registration process is run for both possible positions and the resulting metrics are compared with one another. According to our experiments, the metric exhibits significant difference between the correct and the wrong side. By choosing the side with the lower metric, the correct side can easily be determined.

With the resulting transformation obtained by the registration process the dosimeter position, and therefore the sensor position, can be reliably computed.

Results and Discussion

The images for the linearity test have been exposed with 5 to 360 mAs and constant tube voltage of 28 kV. The template image has been taken with the highest exposure for the reason of better image quality. Our experiments show that, for typical cases, this method identifies the dosimeter and its position correctly. For the dosimeter positioning, we compared the manual procedure with the automated test method and achieved an mean deviation of 9.16 pixels in translation and 2.3° degrees in rotation from the manual method. The standard deviation is 13.56 pixels for the translation and 0.47° for the rotation. In relation to a ROI size of 1420x386 pixels this is sufficiently precise for this application.

The results for the second registration of the characteristic component are 77.00 pixels of mean deviation and 187.30 pixels of standard deviation in translation as well as 2.5° of mean deviation and 0.36° of standard deviation in translation. These results are in relation to a ROI size of about 348x348 pixels. This degree of precision is sufficient to select the correct side of the dosimeter.

The described test framework takes into account all image quality tests from the Siemens Quality Control Manual [8]. Although not all test procedures are applicable to be fully automated, like the DQE, the

operator gains significant assistance by the software in each operation step. This enables the operator to achieve a remarkable improvement in both the test duration and reliability of the results.

Literature

- [1] Barrett H.H., Myers, K.J.: Foundations of Image Science. Wiley Interscience, Hoboken, 2004
- [2] Beutel J., Kim Y., Kundel H.L., Horii S.C., Van Metter R.L.: Handbook of Medical Imaging: Physics and Psychophysics, SPIE Press, 2000.
- [3] Bloomquist A.K., Yaffe M.J., Pisano E.D., Hendrick R.E.: Quality Control for Digital Mammography in the ACRIN DMIST Trial: Part I. Medical Physics, Vol. 33, No. 3. March 2006
- [4] European Commission: European Protocol for the Quality Control of the Physical and Technical Aspects of Mammography Screening. Draft, 2005.
- [5] L. Ibanez, W. Schroeder, L. Ng, J.Cates: The ITK Software Guide. Kitware Inc., second ed., 2005.
- [6] Mayo P., Rodenas F., Verdu G., Villaescusa, J.I., Campayo J.M.: Automatic Evaluation of the Image Quality of a Mammographic Phantom. Computer Methods and Programs in Biomedicine, 73: 115-128, 2004.
- [7] Pachoud M., Lepori D., Valley J.-F., Verdun F.: A new test phantom with different breast tissue compositions for image quality assessment in conventional and digital mammography. Physics in Medicine and Biology, 49: 5267-5281, 2004.
- [8] Siemens AG, Healthcare, Erlangen: Quality Control Manual MAMMOMAT Inspiration VA 10, 2007.
- [9] Unfors Instruments, <http://www.unfors.com>
- [10] Yaffe M.J., Bloomquist A.K., Mawdsley G.E., Pisano E.D.: Quality Control for Digital Mammography: Part II Recommendations from the ACRIN DMIST trial from the ACRIN DMIST trial Medical Physics, Vol. 33, No. 3, March 2006

Affiliation of the first Author

Christoph Heim
Chair of Pattern Recognition,
Department of Computer Science
Friedrich-Alexander-University Erlangen-Nuremberg
Martensstr. 3, 91058 Erlangen, Germany
christoph.heim@informatik.stud.uni-erlangen.de